



Article

CO₂ and Cost Optimization of Reinforced Concrete Cantilever Soldier Piles: A Parametric Study with Harmony Search Algorithm

Zülal Akbay Arama ¹, Aylin Ece Kayabekir ^{1,*}, Gebrail Bekdaş ¹  and Zong Woo Geem ^{2,*} 

¹ Department of Civil Engineering, Istanbul University–Cerrahpaşa, Istanbul 34320, Turkey; zakbay@istanbul.edu.tr (Z.A.A.); bekdas@istanbul.edu.tr (G.B.)

² College of IT Convergence, Gachon University, Seongnam 13120, Korea

* Correspondence: ecekayabekir@gmail.com (A.E.K.); geem@gachon.ac.kr (Z.W.G.)

Received: 25 May 2020; Accepted: 20 July 2020; Published: 22 July 2020



Abstract: This paper presents the parametric modelling process of cantilever soldier pile walls based on CO₂ and cost optimization with the Harmony Search Algorithm. The study attempted to fulfil the geotechnical and structural design requirements and sustainable usage necessities simultaneously. The variants of the optimum design process are selected as the cross-sectional characteristics of cantilever soldier piles such as the length and diameter of the pile, and the other design variables are the reinforcement detailing of the pile such as the diameter and the number of reinforcement bars. Besides the volume of the concrete, the unit prices of both reinforcement and concrete are evaluated as another part of the variants. The shear and flexural strength necessities, minimum cross section of the reinforcing bars and factor of safety values are identified as the constraints of the optimization. Different objective functions are defined to provide the minimum cost, the minimum CO₂ emission and the integrated multi-objective evaluation of cost and CO₂. In addition, the type of steel and concrete reinforcement on the optimum CO₂ emission is investigated with the use of different material emission values that are selected from current literature studies. Consequently, the results of the optimization analyses are interrogated to investigate if the attainment of both minimum CO₂ and cost balance can be achieved.

Keywords: cantilever soldier piles; cost optimization; CO₂ emission optimization; embedment depth; optimization; frictional soils; harmony search algorithm

1. Introduction

The execution of an excavation at the construction sequence makes it necessary to use retaining structures to procure support for ensuring lateral forces that are dependent on the excavation depth and the kind of soil in which it is embedded [1]. Cantilever soldier piles are one of the most preferred retaining structures that are used to resist lateral earth thrusts. Soldier piles present the advantage of penetrating through a wide range of soil types, along with the ease of construction. Besides, the labor costs of soldier piles are significantly lower than other conventional types of retaining structures. In addition, the design process for all retaining structures remains the same, beginning with the determination of lateral active and passive earth pressures to control the stability according to the envisaged dimensions and followed by the fulfillment of structural requirements. Several studies have been conducted up to the present to determine the lateral earth thrust through the excavation and pile depth based on the soil geotechnical properties and the environmental situations [2–6]. In some of these studies, the usage of the resemblance of a pile-soil interacted system with beams on elastic soil is preferred to simplify solutions [4,7–10]. In the application process of these perspectives, stability

analysis is performed based on the beams on elastic soil assumption to obtain the length and diameter of the pile, but it is also required to determine the flexural moment and the shear force of the wall system to complete the structural design. The choice to use reinforced concrete in the design of the pile system is generally economically advantageous. Therefore, the number and diameter of the required reinforcing bars and the volume of the concrete have to be also determined. This order of design steps necessitates an integrated solution to ensure both safety and economy. But current design and application methods related to the literature studies about the design process of cantilever soldier piles providing both geotechnical and structural safety and economic saving are missing. Moreover, in addition to this dual interaction of safety and economy, another significant factor has also been considered mostly in the 21st century due to the effects of global warming. This important factor is the environmental impacts of construction materials that has become a major topic of current research. In connection with this, from the viewpoint of sustainability, construction materials made of reinforced concrete, such as the concrete and steel, cause larger emissions of carbon dioxide which has destructive effects on the environment and increases global warming [11]. Therefore, the amounts of structural materials which are used in the construction process need to be known and projects have to be designed considering carbon dioxide emissions. However, this necessity makes it difficult to solve the complicated phenomenon of designing structures. The minimization of cost, ensuring safety and the minimization of CO₂ emission do not make for an easy problem to solve because of the usage of discrete design variables in the related cases. That is why the use of optimization-based methods for modelling cantilever soldier piles has seemed to be an efficient tool for obtaining the relationship between design safety, cost efficiency and harmless design. The optimization methods generally identify the structure, relying on the design variables, automatically calculated and validated the selected type of the structure, and afterwards redefine the case by the performing process of the algorithm which controls the flow of a large number of iterations in the investigation of the optimum [12]. Especially meta-heuristic search techniques such as Genetic Algorithm [13–16], Particle Swarm Optimization [17,18], Firefly Algorithm [19,20], Big Bang Big Crunch [21,22], Harmony Search [23,24], Bat algorithm [25], Charged System Search [26], Simulated Annealing [27–29], Flower Pollination Algorithm [30] are advantageous to solve the optimization problems of retaining structures. Most of these studies focus on the cost optimization schedule of cantilever retaining wall design problems and none of the studies investigates the optimization problem of cantilever soldier pile walls. In order to overcome this absence in the present study, initially the cost optimization problem and the CO₂ emission problem of piles are taken into account individually, then the integrated relationship of cost and CO₂ minimization is investigated with multi-objective optimization design application. Harmony Search Algorithm, which is adapted from the harmonies of an orchestra and developed by Geem et al., [23] is used to investigate the three-way interaction of design requirements [31]. The Harmony Search Algorithm has been used in many optimization problems, such as real world applications (music composition, sudoku puzzle, timetabling, etc.), computer science problems (web page clustering, visual tracking, robotics, etc.), electrical engineering problems (energy system dispatch, photo-electronic detection, power system design, etc.), civil engineering problems (structural design, soil stability analysis, groundwater management, etc.), mechanical engineering problems (heat exchanger design, offshore structure mooring, etc.), biomedical and medical applications (RNA structure prediction, medical physics and etc.) [32]. Besides, the retaining structure design problem is also investigated by some researchers with the use of the Harmony Search Algorithm [24,33,34] but the topic of integrated analysis of cost and CO₂ emissions is not selected as a case of the studies. Additionally, the cost and CO₂ emission problem of retaining structures are studied by several researchers with the use of different algorithms. Aydoğdu and Akin [11] performed optimization analysis with a biogeography-based optimization technique to obtain cost and CO₂ emission minimization. Yepes et al. [35] used a Black Hole meta-heuristic algorithm along with a discretization mechanism depending on min-max normalization. The geometric variables of the structure and the steel, concrete values were obtained and the results of the analysis were compared with another algorithm that solved the problem. As a result of this study, it is suggested that the

solution which minimizes CO₂ emissions is preferred to use of concrete instead which optimizes the cost. Villalba et al. [12] identified a methodology for designing reinforced concrete cantilever earth retaining walls depending on the minimization of CO₂ emissions with the simulated annealing algorithm. The design variables of the solution were selected as the dimensions of the retaining wall system and reinforcement setups. The results of the analysis show that the embedded emissions and cost are closely related. Aydoğdu [36] used a biogeography-based optimization algorithm to check if it is possible to minimize both cost and CO₂ emission for reinforced retaining walls. The objective functions that are used in the study are formed for determining the minimization of CO₂ emissions and multi-objective functions are defined by generating a special relationship between cost and CO₂ emissions. Eight of the selected design variables are related to the cross-sectional dimensions and five of the design variables are related to the reinforcement details. In addition to these studies, Aydoğdu [36] investigated the effects of steel and concrete classes on the optimization. Khajehzadeh et al. [37] studied a new version of the gravitational search algorithm which depends on the opposition-based learning algorithm to design reinforced concrete walls. Three objective functions are used to relate weight, cost and CO₂ emissions. Five geometric variables and three reinforcement designing variables were selected. A comparison between the newly applied algorithm and a gravitational search algorithm was made. Numerical examples were conducted to show the viability and accuracy of the used algorithm. Öztürk and Türkeli [38] tried to find the minimum cost and CO₂ emissions by using the Jaya algorithm to design retaining walls with a key section at the bottom. Twelve design variables, including the dimensions and reinforcement specifications, are defined. Numerical examples have been conducted to investigate the magnitude of the surcharge load and the effects of soil properties are also studied to search for the relationship between the minimum cost and CO₂ emissions.

In the current study, the optimization application process of the cantilever soldier pile retaining walls is investigated with the use of the Harmony Search Algorithm. The geotechnical design of the cantilever pile system is identified by the beams on elastic soil assumption and the design analysis is continued in order to supply structural requirements simultaneously. Two different objective functions are defined to evaluate cost and CO₂ emission effects on the design individually, and then the integrated influence of both cost and CO₂ emission is evaluated with the definition of two other objective functions in order to obtain an eco-friendly design. The variants of the analysis are selected in relation to both the cross-sectional properties of cantilever soldier piles and also another relation is defined according to the reinforced concrete design requirements. Besides, the constants of the analyses are identified depending upon the related literature sources and manuals. In addition, the excavation depth change is taken into account and different costs and CO₂ emission amounts are defined for structural materials.

This study is original in considering the cantilever soldier pile walls that have not been investigated to a sufficient degree in the literature. At the same time, the eco-friendly design concept of cantilever soldier piles is attempted primarily in the context of present study. As the result of the study, it is aimed to reach the applicability of both cost and CO₂ emission minimization together with the safe design.

2. Design and Methodology

A typical cross section of a single soldier pile is given in Figure 1a. In Figure 1a, z is the depth of excavation, d is the penetration depth of the pile, L is the total length of the pile, D is the diameter of the pile. In Figure 1b, the active and passive stress distribution through the pile are shown depending on the beams on elastic soil assumption. In this study, Rankine's earth pressure theory is selected to use for determining the lateral active and passive earth coefficients K_a and K_p , respectively (Equations (1) and (2)).

$$K_a = \tan^2\left(45 - \frac{\phi}{2}\right) \quad (1)$$

$$K_p = \tan^2\left(45 + \frac{\phi}{2}\right) \quad (2)$$

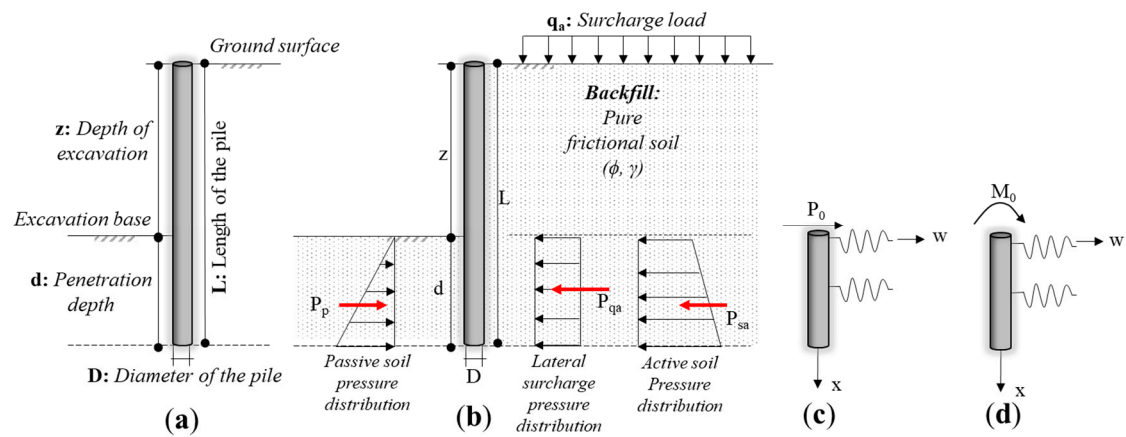


Figure 1. The cross section of a single soldier pile (a); Lateral forces (b); Application of beams on elastic soil assumption (c,d).

In Figure 1b, q_a represents the external surcharge load, which is converted to P_{qa} , lateral surcharge force, by the multiplication of the q_a value with the lateral active earth coefficient. The stability of the pile wall belongs to the generation of the lateral pressures on both sides of the wall [39,40]. In Figure 1, P_{sa} and P_p identify the lateral soil reaction forces of the active and passive state, respectively. Based on the beams on elastic soil assumption, the soldier piles are considered to be located tangentially to form a continuous wall system and the soil formation which has dominated the project site is identified by an elastic continuum [8,9,41,42]. The active and passive reactions of the soil formation at a specified section of the soldier pile are only related to the deformations of the considered part and the reactions are independent of the deflections which have occurred above and below it [8,9]. Accordingly, the penetration depth and the location of the pivot point are only related to the equilibrium of forces that are generated along the embedded section of the soldier pile. The challenging feature of the usage of soil as a continuum can be defined in relation with the defined soil geotechnical parameters that are measurable and realistic like the stiffness and strength [4]. The flexural rigidity of the soldier pile is EI and the characteristic length of the soldier pile is l_0 . In Figure 1c a single lateral force and in Figure 1d a moment has been applied at the edge of the beam.

Hence, the change of the deflection, rotation, bending moment, shear force can be determined with the use of Equations (3)–(6) respectively by the use of the soil reaction coefficient K_s .

$$w(x) = \frac{P_0 l_0^3}{EI} a_{wp}(x) \quad w(x) = \frac{M l_0^3}{EI} a_{mp}(x) \quad (3)$$

$$Q(x) = \frac{P_0 l_0^2}{EI} a_{tp}(x) \quad Q(x) = \frac{M l_0^2}{EI} a_{tp}(x) \quad (4)$$

$$M(x) = \frac{P_0 l_0}{EI} a_{mp}(x) \quad M(x) = \frac{M l_0}{EI} a_{mm}(x) \quad (5)$$

$$V(x) = P_0 a_{vp}(x) \quad V(x) = \frac{M_0}{l_0} a_{vm}(x) \quad (6)$$

Equation (7) is defined to calculate the characteristic length of pile if the coefficient of soil reaction remains constant through the depth and Equation (8) is used in such cases that the coefficient of soil reaction is increasing linearly through the depth.

$$l_0^4 = 4EI/k_f t \quad (7)$$

$$l_0^5 = 4EI/\left(\frac{kb}{x}\right) \quad (8)$$

The penetration length of the soldier pile is calculated by the multiplication of characteristic length of the pile by “ π ” for behaving like a beam supported by elastic soil [8]. Finally, the total length of the soldier pile can be determined by the sum of excavation depth and penetration depth. Within this study, based on the application of beams on elastic soil assumption, the Harmony Search Algorithm is used to model cantilever soldier piles by performing analyses with Matlab software. This special algorithm is proposed as a meta-heuristic algorithm which is inspired from the musical process of the investigation for a perfect state of harmony by Geem et al. [23]. This perfect state can be calculated with the use of an aesthetic standard. The optimization process of the Harmony Search Algorithm investigates the way to obtain a global solution as a perfect state that can be calculated by an objective function [43–45]. The usage of the Harmony Search Algorithm can be defined in five steps. Firstly, a harmony memory starts with the definition of the design constants, the boundary values of design variables, the maximum iteration number and the specific parameters of algorithms such as the harmony memory size (HMS), the harmony consideration rate (HMCR) and the pitch adjustment rate (PAR). A new harmony is concocted from the generation of a harmony vector with the formation of a random value ($rnd(0,1)$) within an envisaged range. The upper and lower boundaries ($X_{i,max}$, $X_{i,min}$) of each design variable (X_i) are defined with Equation (9). The motion equation is calculated by the use of the design constants and variables of the related problem. The solution of the defined objective function is achieved and the results are stored in the harmony vector. This application is repeatable directly proportional to the size of the harmony memory. All the harmony vectors are stored in a matrix that is called the initial solution matrix.

$$X_i = X_{i,min} + rnd(0,1) \cdot (X_{i,max} - X_{i,min}) \quad (9)$$

In the next step, the iteration process is started and the new harmony vector is generated. The algorithm rules are applied for the acquirement process of the new harmony vector by using two different choices. The upper and lower boundaries are used as boundaries to generate the design variables randomly in the first choice or for the second choice, it is possible to use a new vector that can be generated with the use of a selected vector ($X_{i,old}$) from the matrix of solution (Equation (10)). During the loading process, the new values ($X_{i,new}$) are formed randomly by the multiplication difference of the pitch adjusting rate (PAR) and the design variable limits.

$$X_{i,new} = X_{i,old} + rnd(0,1) \cdot PAR \cdot (X_{i,max} - X_{i,min}) \quad (10)$$

The HMCR value is used to obtain the new vector by the selection of the appropriate way of solving the equation. As a result, the generation of a random value occurs and if the HMCR value becomes larger than the random value, the first choice is selected; if not, the second choice is applied. The fourth step includes the comparison of the new vector with the vectors that are stored in a solution matrix. Interrelating with the objective function, a new vector is used instead of the existing vector on condition that the next vector is better than the existing one. If not, the current form of the solution matrix is saved. The minimum value of the solutions is selected to evaluate the best one through the comparison of the values attained from the objective function. The constraints of the design are also considered in the comparison process. Besides, the number of the violations is controlled and the solution including the minimum violation is chosen to be the best even if violations of the design constraints exist. The last step is the control of the stopping criterion. Iterations are stopped if the satisfaction of the stopping criterion is supplied. Different ways are used to define the stopping criterion, but in the context of the study, it is calculated as the maximum iteration number.

In order to solve the cantilever soldier pile problem, three design parameters are defined. The diameter of the soldier pile (X_1) is the selected variable that is in relation to the cross-section dimension, and the diameter of the reinforcing bars and their numbers (X_2 , X_3) constitute the variables that are in relation to the reinforced concrete. The variables of the soldier pile wall design are given in Table 1. The requirements of the reinforced concrete design are defined based on American Concrete

Institute design code (ACI 318-05) [46]. This code suggests to model equivalent rectangular compressive stress distribution. The use of this suggestion leads to determining the moment capacity of the cross section of the pile. The flexural moment is represented by M_u , the shear force is V_u , the area of the reinforcing bars is A_s and the diameter of the reinforcing bars is ϕ_p .

Table 1. The variables of the cantilever soldier pile design.

	Symbol	Description of Parameter
Variables in relation to cross-section dimension	X_1	Diameter of soldier pile (D)
Variables in relation to reinforced concrete design	X_2	Diameter of reinforcing bars of soldier pile (ϕ_p)
	X_3	Number of reinforcing bars of soldier pile

The design constraints that are used in the solution of the cantilever soldier pile wall problem are given in Table 2.

Table 2. Design constraints of the solution.

Description	Constraints
Flexural strength capacities of critical sections (M_d)	$g_1(X): M_d \geq M_u$
Shear strength capacities of critical sections (V_d)	$g_2(X): V_d \geq V_u$
Minimum reinforcement areas of critical sections (A_{smin})	$g_3(X): A_s \geq A_{smin}$
Maximum reinforcement areas of critical sections (A_{smax})	$g_4(X): A_s \leq A_{smax}$

This study is focused on four main aims of the design process of cantilever soldier piles:

- i. The stable design of cantilever soldier pile walls;
- ii. Cost minimization-based design of cantilever soldier piles;
- iii. CO₂ emission minimization-based design of cantilever soldier piles;
- iv. Both cost and CO₂ minimization-based design of cantilever soldier piles.

The difference reveals the need to define purposive objective functions to obtain accurate results. Therefore, in the context of this study, four different objective functions are used.

The first objective function aims to design the pile wall system with dual integration of both stability and cost minimization. The suggested first objective function consists of four main variants such as the unit cost of the concrete $C_{c,cost}$, the volume of concrete V_c , the unit cost of reinforcing bars $C_{s,cost}$ and the unit weight of reinforcing bars W_s . The mathematical expression of the first objective function can be determined by Equation (11).

$$f_{cost}(X) = C_{c,cost} \cdot V_c + C_{s,cost} \cdot W_s \quad (11)$$

The second objective function aims to design the pile wall system with dual integration of both stability and CO₂ emission minimization. The proposed second objective function includes four main variants such as the CO₂ emission caused by the production process of unit volume of concrete $C_{c,co2}$, the volume of concrete V_c , the CO₂ emission caused by the production process of a unit weight of steel $C_{s,co2}$ and the unit weight of reinforcing bars W_s . The mathematical expression of the second objective function can be determined by Equation (12).

$$f_{co2}(X) = C_{c,co2} \cdot V_c + C_{s,co2} \cdot W_s \quad (12)$$

The third objective function aims to design the pile wall system with a three-way integration of stability and cost and CO₂ emission minimization. The suggested third objective function includes four different variants such as the weight multiplier of cost ξ_{cost} , the weight multiplier of CO₂ emission

ξ_{CO_2} , the cost of the design f_{cost} and the CO₂ emission which is obtained in cases when the cost of the design is f_{co2} . The weight multipliers are selected at 0.5 for this study to reflect an equal participation rate of both cost and CO₂ emission. This function has been proposed in a way that allows to compare the cost and CO₂ emission amounts expressed in two different units. The mathematical expression of the third objective function can be determined by Equation (13).

$$f_{ag}(X) = \xi_{cost} \ln(f_{cost}) + \xi_{co2} \ln(f_{co2}) \quad (13)$$

The last objective function aims to design the pile wall system with a three-way integration of stability and cost and CO₂ emission minimization as the third objective function. This function is taken as an example from the studies of Aydoğdu and Akin to simplify comparisons [11]. The suggested fourth objective function includes two non-negative weights considering both cost (ξ_{cost}) and CO₂ emission (ξ_{CO_2}) which are taken as 1 for this study. The mathematical expression of the fourth objective function can be calculated by Equation (14).

$$f_{ag}(X) = \xi_{cost} f_{cost} + \xi_{co2} f_{co2} \quad (14)$$

3. Parametrical Analyses

In order to exemplify the optimization process of cantilever soldier pile walls, which are embedded in pure frictional homogenous soil formation, parametrical analyses were performed with the use of the Harmony Search Algorithm. The investigations are focused on the changes of cost, CO₂ emission and their interaction with arbitrarily selected various excavation depths. The design of the cantilever soldier piles has changed according to the excavation depth as expected. The integrated alteration of relationships was also studied by using the different unit costs and CO₂ emissions of the concrete and steel materials. The aim was to find the interaction if it would be possible to ensure both cost saving and minimum CO₂ emissions with the same design dimensions which provide geotechnical safety and fulfil the structural requirements simultaneously. The design variables and the constants of the envisaged cases are shown in Table 3. The depth of excavation was selected to be between 4–12 m, depending on the application limits of cantilever retaining structures in projects and based on national and international sources [47–50]. The piles were embedded into pure frictional homogenous soils in which they had a shear strength angle of 30° and the unit weight of the soil was 18 kN/m³. The characteristic length of the pile was determined with the use of the coefficient of soil reaction which was selected to be 200 MN/m³ [1].

Table 3. The design constants and the design variables.

Symbol	Definition	Value	Unit
h	Depth of excavation	4 to12	m
f_y	Yield strength of steel	420	MPa
f'_c	Compressive strength of concrete	30	MPa
c_c	Concrete cover	30	mm
E_{steel}	Elasticity modulus of steel	200	GPa
$E_{concrete}$	Elasticity modulus of concrete	23.5	GPa
γ_{steel}	Unit weight of steel	7.85	t/m ³
$\gamma_{concrete}$	Unit weight of concrete	25	kN/m ³
C_c	Cost of concrete per m ³	50, 75, 100, 125, 150	\$
C_s	Cost of steel per ton	700, 800, 900, 1000, 1100	\$
q	Surcharge load located adjacent the top of the pile	10	kPa
β	Backfill slope angle	0	°
ϕ	Shear strength angle	30	°
γ	Unit weight of soil	18	kN/m ³
D	Diameter of pile	0.3–2	m
ϕ_p	Diameter of reinforcing bars of soldier pile	14–40	-
n	Number of reinforcing bars of soldier pile	6–20	-

In addition, it was assumed that an infinite uniformly distributed load (surcharge load) should be applied to the top of the backfill side. The magnitude of the surcharge load was selected to be constant (10 kPa) for all the conducted example cases. The unit costs of the structural materials were also selected as changeable. The unit cost of the concrete per m³ was selected at \$50, \$75, \$100, \$125 and \$150 and the unit cost of the steel of the reinforcing bars per ton was selected at \$700, \$800, \$900, \$1000 and \$1100.

Besides, the CO₂ emission amounts were also selected as different values based on literature sources [22,51,52]. The selected different emission values were used to perform analysis with the use of objective functions 2, 3 and 4. Based on these values, three different cases were arranged. The variable CO₂ emission values and their references are listed in Table 4. Yeo and Potra [51] proposed to use a CO₂ emission amount of 376 kg for concrete which has 30 MPa strength and suggested to use a CO₂ emission amount of 352 kg for recycled types of steel with 420 MPa strength. Paya et al. [52] proposed to use 3010 kg for the CO₂ emission amount of steel and the CO₂ emission amount of 143.48 kg for concrete (HA-30) which has 30 MPa strength. The selected amounts of emissions approximately represent the upper and lower boundaries of the available amounts used in the literature studies.

Table 4. Unit rates for CO₂ emissions of structural materials.

Material	Class	Case 1	Case 2	Case 3
Concrete	C30	376	143.48	143.48
Steel	S420	352	3010	352

4. Result and Discussion

Depending upon the mentioned parametric analysis details, a great number of numerical analyses were performed with the Harmony Search Algorithm. The results of the analyses are divided into three main parts according to the solutions of objective functions to provide expression integrity. The first part of the analysis includes the solutions of objective function 1 to discuss the effects of cost on the design. The second part of the analysis combines the solutions of objective function 2 to discuss the CO₂ emission effects of retaining piles and to show the effects of CO₂ emission on the design of piles. Furthermore, three different cases are conducted in order to examine the effects of the change of CO₂ emission amounts. The third part of the analysis includes the solutions of both objective function 3 and 4 to present the integrated relationship between design, cost and CO₂ emissions to ensure a sustainable design. Consequently, a total of 2251 analyses were performed to query the necessities of design to attain an eco-friendly solution. The results are illustrated with graph systems and C_t represents the total cost of the pile system for unit width, D is the diameter of the pile, z is the excavation depth, L is the total length of the pile, C_c is the unit cost of the concrete per m³, C_s is the unit cost of the steel per kg, ϕ is the diameter of reinforcing bars, n is the number of reinforcing bars for all the illustrated graphs.

4.1. Design and Minimum Cost Relationship

Equation (11) is used to examine the relationship between the changes of design according to the cost of materials. The results are arranged to discuss the change of unit costs of structural materials in the design. Figure 2 is illustrated to present the effects of concrete unit cost change in the design. Therefore, the unit cost of the steel is assumed to be constant at \$700 and the unit cost of concrete is increased step-by-step. In Figure 2a, the change of total cost via the change of excavation depth is shown according to the increment of unit cost of concrete. The increase of the concrete costs raises the total cost of the pile system as expected. The increase of the concrete cost by three times more than the smallest cost value leads to increasing the total cost of the pile wall system two times more than the smallest cost obtained within this study. As a result, it is obvious that the unit cost of the concrete is directly proportional to the total cost of the system. Besides, it is clear to see that the increase of the excavation depth also induces the increment of the total costs. Figure 2b represents the change of total pile length against the increase of excavation depth. The increase of excavation depth requires to

lengthen the pile due to the stability requirements. Figure 2c shows the change of pile diameter against the change of total pile length. In such a case it would be true to say that the stability requirements can be ensured by both lengthening and enlarging the pile section if the increase of the excavation depth is possible. In addition, a linear increase can be seen from Figure 2 which increases the ratio of both the diameter and the length of the pile.

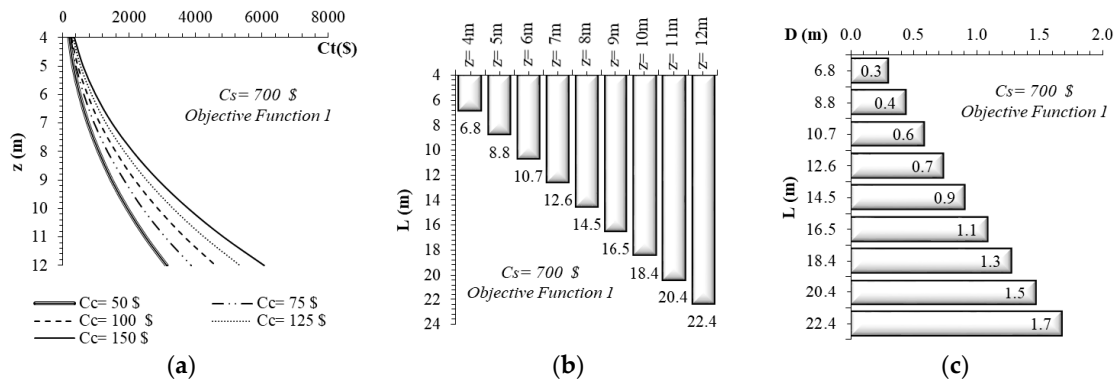


Figure 2. (a) The change of total cost against the excavation depth and concrete cost; (b) The change of total pile length against the excavation depth; (c) The change of pile diameter against the pile length.

Figure 3 reflects the number and diameter of the reinforcing bars used to construct the pile wall. This case is prepared for arbitrarily selected constant values of unit costs of concrete and steel. The unit cost of the concrete is selected at \$50 and the unit cost of the steel is assumed to be \$700. In Figure 3a, except for 7–8 m excavation depth, the increase of the diameter of the reinforcing bars against the excavation depth or the pile length can be seen. In Figure 3b, there cannot be seen a direct linear relationship between the depth of excavation and the number of the reinforcement. But it can be said that 7–8 m excavation depths may generate a boundary length for ensuring the stability requirements. The number of the reinforcing bars remains the same until the length of 12.6 m (8 m excavation depth) but the diameter of the bar increases unexpectedly. After this boundary length the diameter of the reinforcing bars has increased linearly, and the number of the bars has stayed approximately the same. This condition may occur depending on the optimization process of the pile design. Some literature sources and manuals have pointed to a special situation about the applicable length of the cantilever pile walls [1,2,46,49,50]. The applicable length of the cantilever soldier pile walls is generally suggested to be between 4–8 m, excluding the penetration depth. The deeper excavations need additional supporting systems such as struts, due to the huge increase of lateral soil thrust. But nowadays, the increase of pile application studies and project requirements makes it necessary to use cantilever soldier piles for deeper excavations. In such a case, the adequate resistance and safety degree of the system can be ensured by increasing the structural resistance with the used materials’ increased strength.

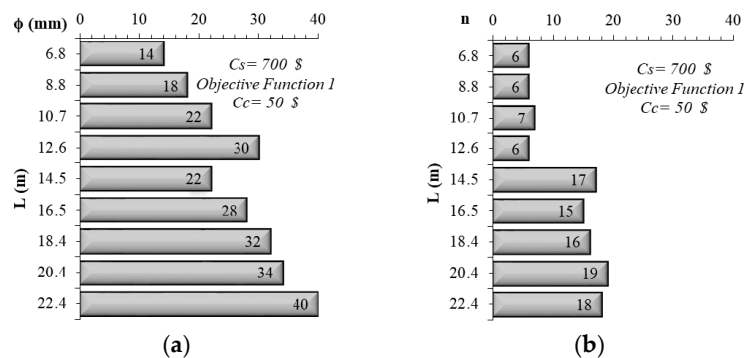


Figure 3. (a) The change of the diameter of reinforcing bars against the total length of pile; (b) The change of the number of reinforcing bars against the total length of pile.

Figure 4 represents the change of the diameter and number of reinforcing bars against the depth with the unit cost of the concrete. The unit cost of the steel is assumed to be constant for these analyses. The increase of the excavation depth increased the required material volume. So, the piles are lengthened and enlarged with the deepening of the excavation depth. The increase of the unit cost of the concrete has not got a significant influence on the number and diameter of the piles except for the depths between 7–9 m. The diameter of the reinforcing bars is increased suddenly at the depth of 8 m, but the number of the reinforcing bars still remains the same. This is the same situation as in Figure 3.

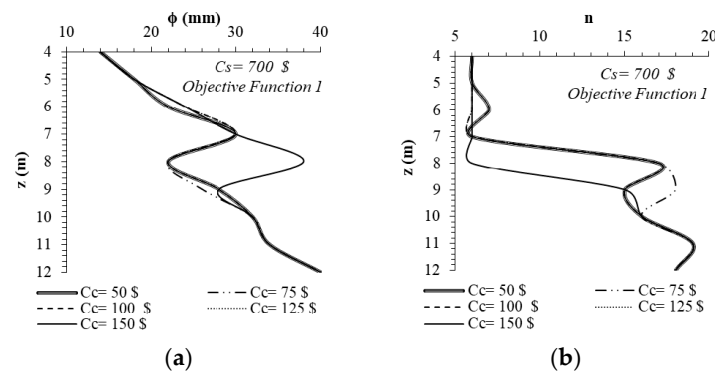


Figure 4. (a) The change of the diameter of reinforcing bars against the excavation depth with the unit cost of concrete; (b) The change of the number of reinforcing bars against the excavation depth with the unit cost of concrete.

In order to evaluate the effects of the unit cost of the steel bars, similar type analyses have been conducted as in the above section. In these analyses, the unit cost of the concrete is assumed to be constant at the amount of \$50. In Figure 5a, the total cost change is evaluated with the change of the excavation depth and the unit cost of the steel. The axes of Figure 5a are selected to be identical to those in Figure 2a to ease comparison. The effect of the steel cost change is less effective than the cost change of concrete. It is because that the necessary volume of the concrete has to be bigger than the steels according to the structural design requirements. In addition to these, in this study, the assumed change of the concrete materials unit cost rate is bigger than the change of the steel materials cost rate. This condition is also effective in the result of this search but it is not an unexpected situation that the most influential parameter of the total cost is the cost of the concrete material. Figure 5b illustrates the total length of the pile against the excavation depth, and Figure 5c shows the diameter of the pile against the total pile length. The change of the total pile length and diameter remains constant with the change of the unit cost of the concrete material. The increase of the unit cost of the steel has not got an influencing effect on the pile dimensions.

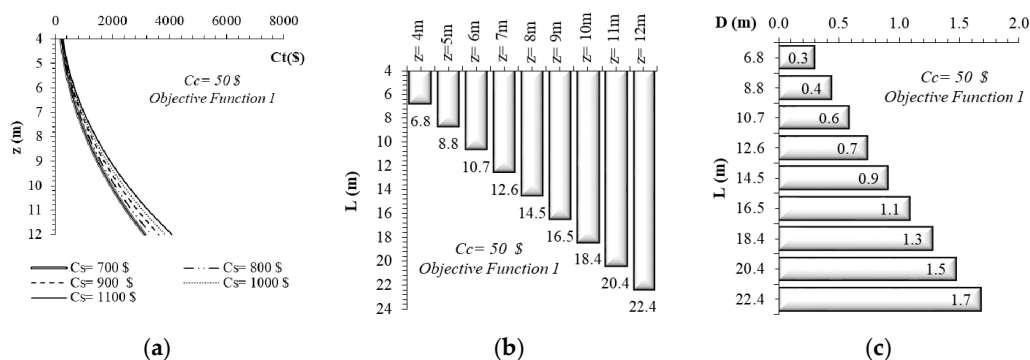


Figure 5. (a) The change of total cost against the excavation depth and steel cost; (b) The change of total pile length against the excavation depth; (c) The change of pile diameter against the pile length.

Figure 6a,b is drawn to present the change of the reinforcing bar diameters and numbers against the total pile length. The unit cost of the steel is assumed to be constant at the highest value of the selected costs (\$1100). Different combinations of the unit prices of steel and concrete are also tested and finally the results show that the change in the steel unit cost has no effect on the reinforcement design. The direct demonstration of this result can also be seen in Figure 7.

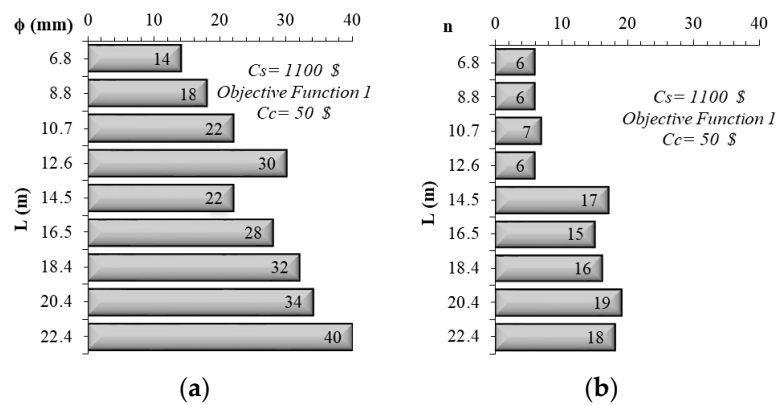


Figure 6. (a) The change of the diameter of reinforcing bars against the total length of pile; (b) The change of the number of reinforcing bars against the total length of pile.

The change of the reinforcing bars’ diameter and number against the excavation depth with the change in unit cost of steel are given in Figure 7. Although the increase in the costs of the steel material, the number and diameter of the reinforcing bars still remain approximately the same as the smallest excavation depth analyses. However, it is a significant point to focus on the “increasing diameter-decreasing number” change at the 8 m excavation depth. Previous studies of the authors have also verified that the 8 m excavation depth constitutes a boundary condition for geotechnical stability. Geotechnical stability conditions cannot be obtained for excavation depths bigger than 9 m in geotechnical analysis, but in this study, the use of optimization algorithms provides an opportunity to utilize both geotechnical and structural stability necessities together and ensures that the wall can resist lateral forces with reinforced concrete design details [53]. Besides, it is a crystal clear fact that the optimization analysis gives more optimistic results.

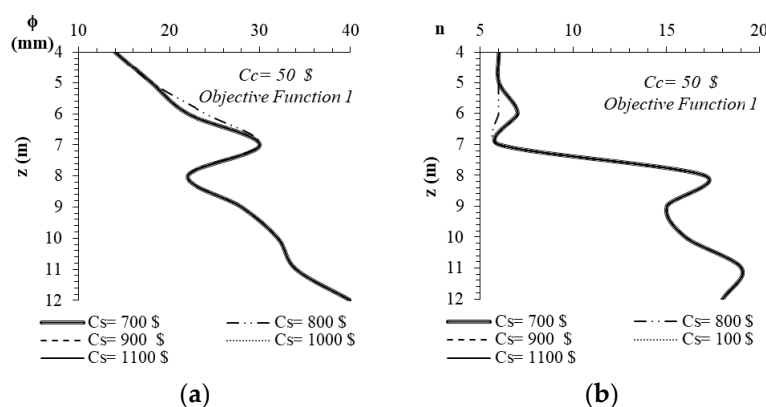


Figure 7. (a) The change of the diameter of reinforcing bars against the excavation depth with the unit cost of steel; (b) The change of the number of reinforcing bars against the excavation depth with the unit cost of steel.

4.2. Design and Minimum CO₂ Emission Relationship

Equation (12) is used to investigate the relationship between the changes of design according to the CO₂ emission amounts of the structural materials. Equation (12) represents objective function 2 of

this study and this objective function is independent of the costs of the structural materials. The results of the analyses are arranged to discuss the change of CO₂ emission variation in the design. In the context of this part, three different cases are analyzed depending on the differences of CO₂ emission amounts for both steel and concrete.

Figure 8a illustrates the results of Case 1 and represents the change of CO₂ emission against the total pile length. The increase of the total pile length leads to an increase in CO₂ emission amounts depending on the excessive volume of the materials used for construction. The change of the total pile length against the excavation depth is also given in Figure 8b. In such a situation, it will be true to say that the increase trend of pile length reflected the increase ratio of CO₂ emission.

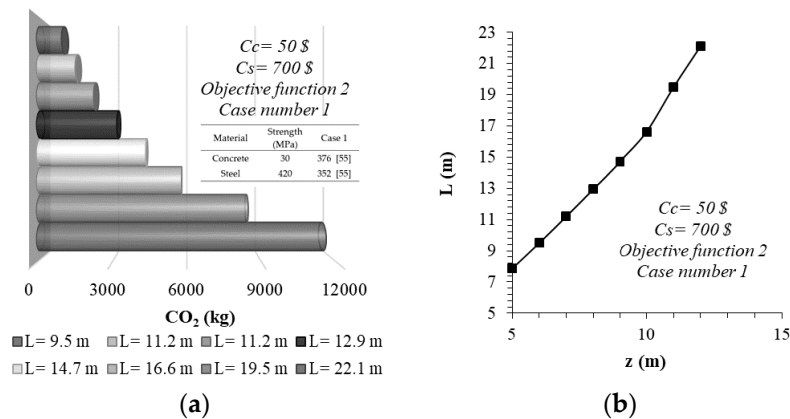


Figure 8. (a) The change of CO₂ emission amount against the total pile length; (b) The change of total pile length against the excavation depth.

Figure 9 shows the change of CO₂ emission amounts against the pile diameter and total length of the pile. In Figure 9a–c, they are arranged with the use of the same numerical values on the axes to ease the comparison. In Figure 9a–c, the results of Case 1, Case 2 and Case 3 are evaluated, respectively. In addition to all of these, in Figure 9, the lateral axes of the graph represent the excavation depths between 4 and 12 m, respectively. In Figure 9a, the increase of the excavation depth causes the diameter of the pile to enlarge. The enlargement of the pile in such a case that the excavation depth is 12 m occurs approximately five times more than the lower boundary of the diameter design, although the increase of the excavation depth is three times bigger than the beginning depth. The increase ratio of the total pile length is directly proportional to the increase of the excavation depth. The increase of the excavation depth is three times more than the beginning depth which causes the total pile length to rise at 12 m excavation, three times more than the pile length obtained for 4 m excavation. In other words, the relative difference ratio between the lower and upper boundaries of excavation depth is the same as the relative difference between the acquired values of the total pile length. The CO₂ emission amounts which are determined for 4 m and 12 m excavation depth respectively are 1007.0 and 11549.6 kg. The increasing amount of CO₂ emissions is not a one-dimensional problem so the increase ratio of the CO₂ emission does not progress like the increase ratio of the pile length or the pile diameter. Therefore, the high rate of increase of CO₂ emissions may be related to the total volume of the pile and the materials that are used to construct the structure. In Case 1, the amount of CO₂ emissions of concrete materials used the biggest value of the selected ones and, in contrast, the amount of the CO₂ emission of steel material used the smallest value of the selected ones. The second selected amount of emissions of steel material is 3010 kg and this value is approximately 8.5 times larger than the first one. It is thought that the relative differences between these two values are caused by the content of the steel. Recycled steel is used for low emission values in the studies of Yeo and Potra [51].

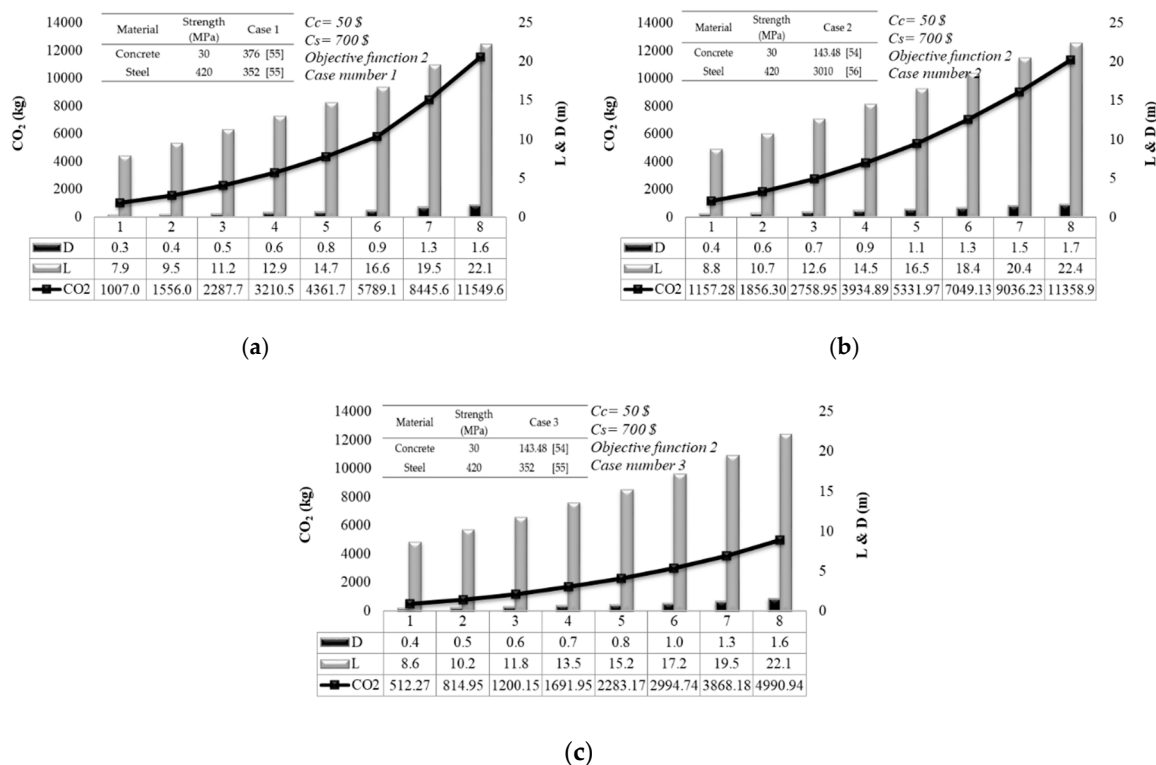


Figure 9. The change of CO₂ emission amount against the pile diameter and total length (a) Case number 1; (b) Case number 2; (c) Case number 3.

In Figure 9b, the lowest amount of emissions for the concrete material and the highest amount of emissions for steel are used. The relative difference between the lowest and highest values of the emission for concrete material is nearly 2.5. The second value of the concrete CO₂ emissions is smaller than the first one. In such a case, it can be seen that the diameter of the pile is affected after 4 m excavation depth when a comparison is made with Case 1. In Case 2, the diameter of the pile has increased, but on the contrary the length of the pile has decreased according to Case 1. In Case 3, the lowest values of the CO₂ emission of both the concrete and the steel materials are used. Although the amount of the CO₂ emission of concrete material in Case 1 is bigger than the amount used in Case 3, the diameter of the pile nearly remains the same for both cases. However, especially for the excavation depths equal to and smaller than 9 m, the total length of the pile increased in Case 3. The decrease of the CO₂ emission of both structural materials leads the total emission to reduce significantly. The relative difference between the emissions of Case 1 and Case 3 shows the effect of concrete CO₂ emission fundamentally. The decrease of the concrete emission in half leads to a reduction of the total emission value at nearly the rate of 50% for 4 m excavation depth. Besides, the decrease of the concrete emission in half leads to a reduction of the total emission value nearly at the rate of 43% for 12 m excavation depth. The relative difference between the emissions of Case 2 and Case 3 shows the effect of steel CO₂ emission fundamentally. The decrease of the steel emission at a 1/8 ratio leads to a reduction in the total emission value of a structure nearly at the rate of 44% for both 4 and 12 m excavation depths.

In Figure 10, the change of pile length, number and diameter of reinforcing bars against the depth of excavation are given. Figure 10a–c is illustrated for 5, 7 and 10 m excavation depths, respectively. On the other hand, the unit costs of the concrete and steel material are assumed to be constant at \$50 and \$700, respectively. The increase of the excavation depth causes to raise the diameter of reinforcing bars, but this condition is not acceptable for the number of reinforcements. The number of reinforcing bars remains the same for 5 and 7 m excavation depths, but when the excavation depth passes 7 m, the number of the reinforcing bars raises unexpectedly.

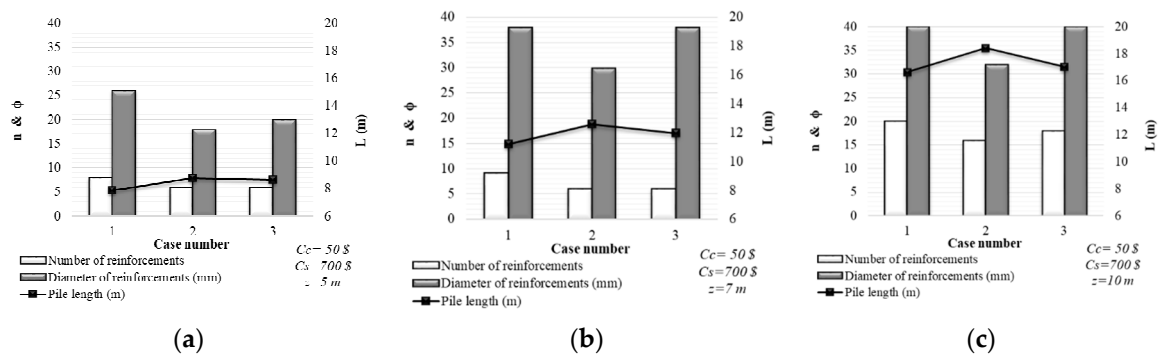


Figure 10. The change of pile length, number and diameter of reinforcing bars against the depth of excavation ($C_c = \$50$ and $C_s = \$700$) (a) $z = 5$ m condition; (b) $z = 7$ m condition (c); $z = 10$ m condition.

In Figure 11, the change of pile length, number and diameter of reinforcing bars against the depth of excavation is given. The unit costs of the concrete and steel material is assumed to be constant at \$150 and \$1000. The comparison of Figures 10 and 11 shows that the change of material costs affects neither the dimensions of the wall nor the reinforcement requirements.

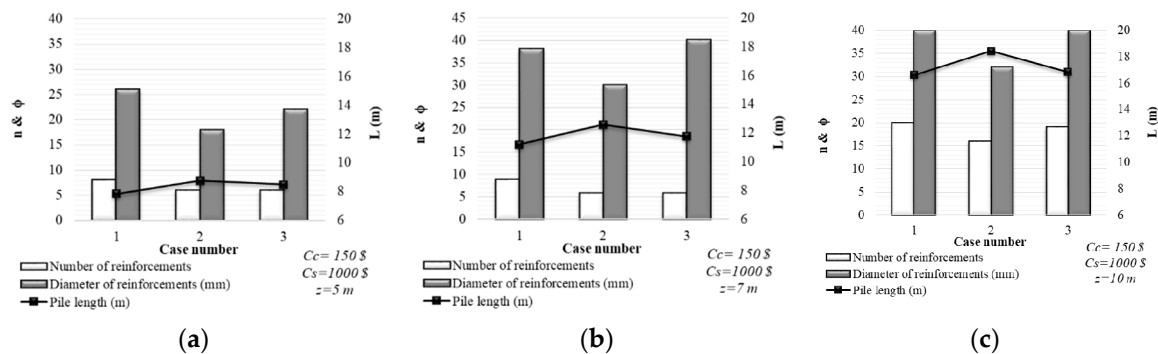


Figure 11. The change of pile length, number and diameter of reinforcing bars against the depth of excavation ($C_c = \$150$ and $C_s = \$1000$) (a) $z = 5$ m condition; (b) $z = 7$ m condition; (c) $z = 10$ m condition.

4.3. Design and Minimum Cost and Minimum CO₂ Emission Relationship

The interactive relationship of optimum design, minimum cost and minimum CO₂ has been defined with the use of two different objective functions. The first objective function is expressed mathematically by Equation (13) and the second objective function is expressed mathematically by Equation (14). In the context of this study, the aforementioned first function is represented by objective function 3 and the previously mentioned second function is represented by objective function 4. The generation reasons of objective function 3 and objective function 4 are related to the evaluation process of the interaction between the total cost and CO₂ emission. This interaction is defined by authors in a special way with the use of objective function 3. It is a well-known issue that the total cost and the CO₂ emission values do not have the same units. So, it will be complicated to state these notions with a total sum. In order to eliminate these unit problems of the notions, it has been thought to determine a log-based equation. In the solution process of objective function 3, the cost and CO₂ emission values are logarithmically stated (ln) and weight multipliers are used to calculate the ultimate sum. Besides, the aim of objective function 4 is the same as that of objective function 3. But the statement way of objective function 4 is differentiated from objective function 3. Non-negative weights are multiplied by the pure values of both cost and CO₂ emission to determine the result of objective function 4. According to Aydođdu and Akin [11] these non-negative weights are assumed to be equal to 1.0. In this study, the assumption of Aydođdu and Akin is approved to conduct all of the envisaged cases. The results of objective function 3 and objective function 4 are attained for both Case 1, 2 and 3 respectively. The acquired results of objective function 3 and 4 are examined with the use of

special constant values of material costs to ease the understandability. In Figure 12, the relationship between the total cost and CO₂ emissions is investigated according to the cases and the unit cost of the concrete and steel are assumed to be \$50 and \$700, respectively. These cases are arranged based on different CO₂ emission values for both steel and concrete as mentioned above. The total cost of all the cases has remained the same because the cost of the whole system was minimized depending on the optimization process and the cross section of the pile was not changed according to the changes of the emission values. The minimization process of the cross section leads the pile to generate minimum CO₂ emission as known. In this connection, it is important to construct the structural systems with the materials which are environmentally friendly. Figure 13 represents the change of both the cost and CO₂ emissions depending on the cases for a different couple of cost values of concrete and steel. The material cost of the concrete is assumed to be \$150 and the cost of the steel material is assumed to be \$1100. The comparison of Figures 12 and 13 shows that the change in material cost has no effect on the values of CO₂ emission but highly raises the ultimate costs of the system. As a result, the contribution of the total cost value in the interacted effect of both cost and CO₂ emission is increased based on the increase of material costs. Especially in the third case, the effect of the cost becomes bigger than the effect of CO₂ emission based on the use of smallest emission values in the solution of the objective function.

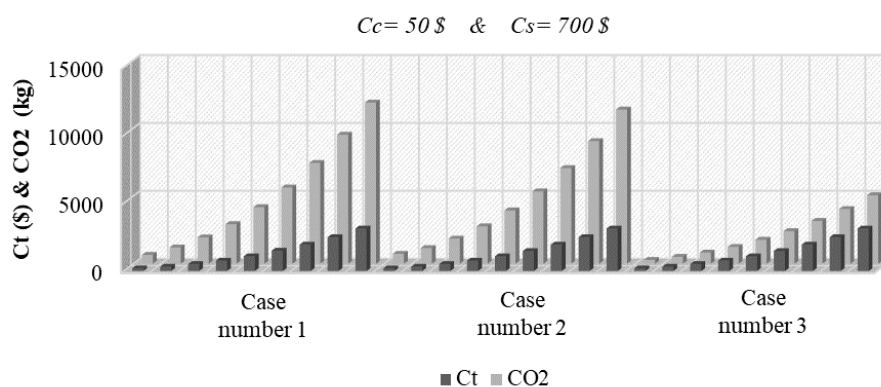


Figure 12. The relationship between the total cost and CO₂ emission ($C_c = \$50$, $C_s = \$700$).

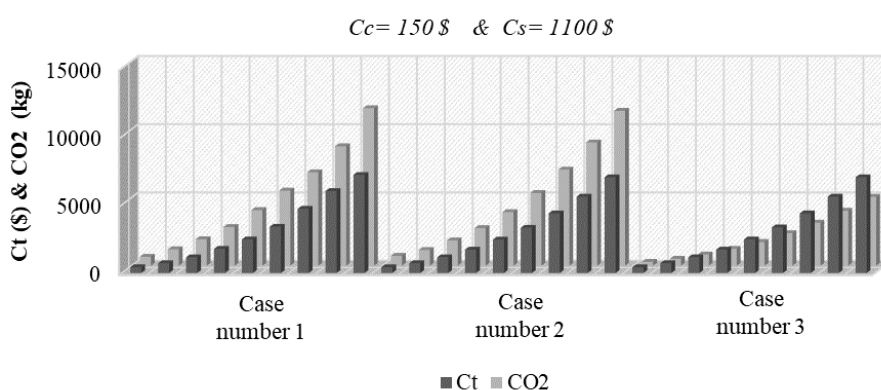


Figure 13. The relationship between the total cost and CO₂ emission ($C_c = \$150$, $C_s = \$1100$).

Figure 14 is given to evaluate the relationship between the pile diameter, pile length and the CO₂ emission value with the use of constant material costs ($C_c = \$50$, $C_s = \$700$) based on the solution of objective function 3. The increase of the total length of the pile causes an increase in the CO₂ emission values as expected. The increase of the pile diameter happens at a slower rate as the increase of the pile length because of the dimensional constraints and structural requirements. Within Case 2, the increase of the emission of steel while the decrease of the emission of concrete balances each other and the total emission values are not changed too much in comparison with the Case 1. However, in Case 3,

the decrease in both material emission values leads to a reduction in CO₂ emissions approximately in half in comparison with the other cases, although the material dimensions remain the same.

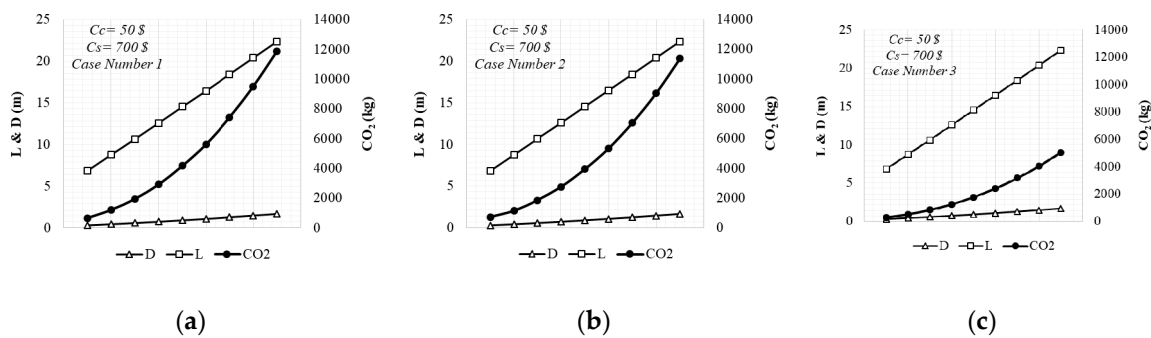


Figure 14. The relationship between the length and diameter of the pile and CO₂ emission ($C_c = \$50$, $C_s = \$700$) (a) Case 1; (b) Case 2; (c) Case 3.

Figure 15 shows the relationship between the number and diameter of reinforcing bars and CO₂ emissions for different excavation depths. The costs of the materials are also assumed to be constant ($C_c = \$50$, $C_s = \$700$) and evaluations are conducted for all the cases in Figure 15. The numbers and diameters of the designed piles remain constant for the cases suggested for the same excavation depths. However, the comparison of Figure 15a,b shows the increase of excavation depth from 5 m to 7 m leading to an increase in the diameter of the reinforcing bars; however, in such a case the number of the bars remains the same. The comparison of Figure 15b,c presents that an increase of the excavation depth from 7 m to 10 m leads to an increase in the number of the reinforcing bars but the diameter of the bars remain the same. The comparison of Figure 15a,c shows that the increase of excavation depth from 5 m to 10 m leads to an increase in both the diameter and number of reinforcing bars. This sequence also represents the logic of the optimization process. It is first tested whether the required strength can be met by the increase of the diameter of reinforcing bars to remain the total cost constant, because in the context of this study the cost differences that can occur depending on the diameter of the bars are not taken into account. In case the structural strength requirements cannot be achieved with the increase of the depth of excavation, it is attempted to provide them by increasing both the diameter of the reinforcement and the number of reinforcements. This situation causes an increase in both cost and CO₂ emissions significantly. In addition to these, the direct proportional relationship of both the excavation depth-pile length and CO₂ emissions can be distinguished through the comparison of the subdivisions of Figure 15.

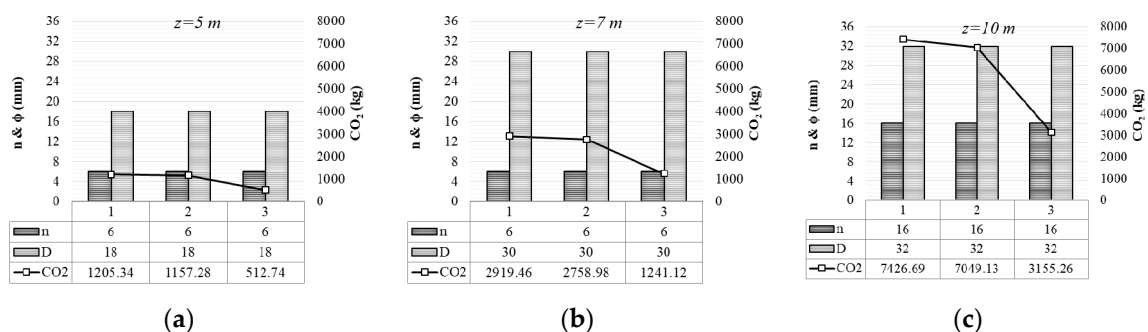


Figure 15. The relationship between the number and diameter of the reinforcing bars and CO₂ emission: (a) $z = 5$ m; (b) $z = 7$ m; (c) $z = 10$ m.

In Figure 16, the results of the objective function analyses are shown. The solution of objective function 4 is based on the studies of Aydođdu and Akin [11]. The arithmetic values of the cost and CO₂ emissions are directly multiplied with the non-negative weights that are assumed to be 1.0 in the

context of the paper of Aydođdu and Akin. The same assumption is used to perform the optimization process of the present study and Figure 16 is compiled to understand the change in total cost and CO₂ emission values based on the depth of excavation, and it also reveals the contribution ratios of cost and CO₂ emission to the ultimate sum. In Figure 16, the contribution of total cost is smaller than the contribution of the CO₂ emission for all cases. However, the effect degree of total cost to the ultimate sum is changed depending upon the cases. The rate of contribution of the total cost to the ultimate sum is determined at 32% maximum for Case 1 (Figure 16a), 21% maximum for Case 2 (Figure 16b), 42% maximum for Case 3 (Figure 16c).

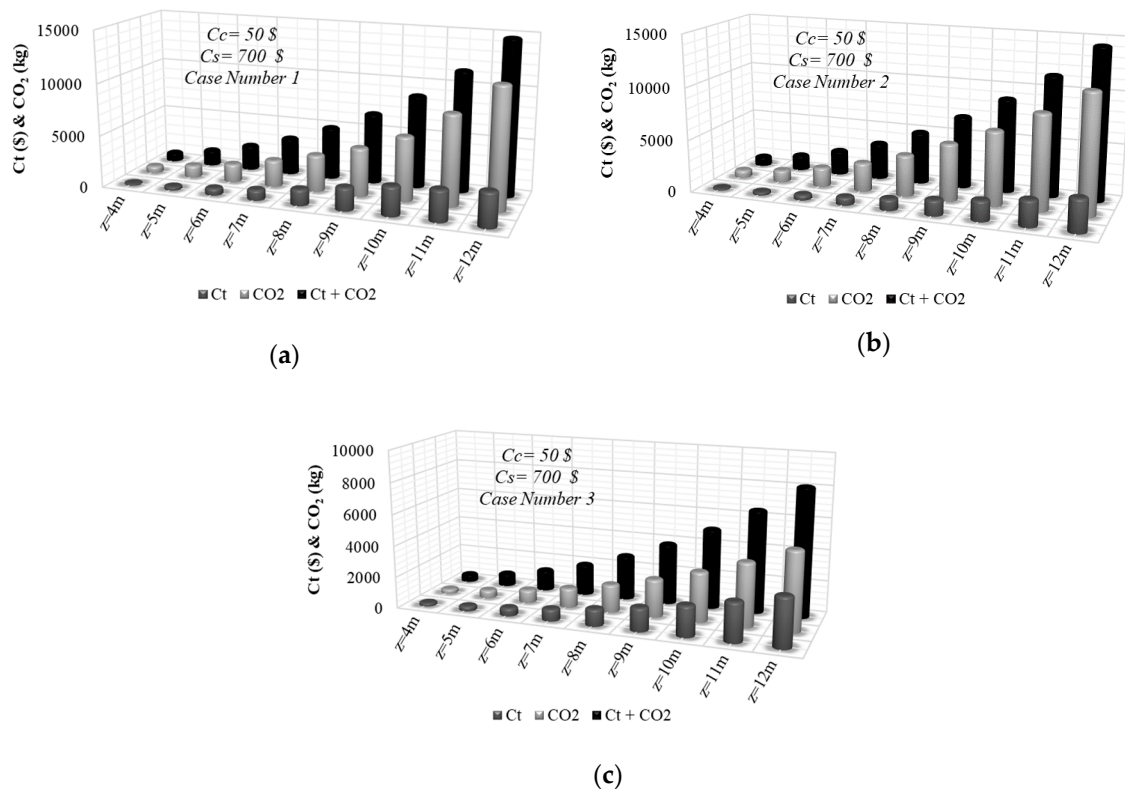


Figure 16. The change of total cost and CO₂ emission based on objective function 3 ($C_c = \$50$, $C_s = \$700$) (a) Case 1; (b) Case 2; (c) Case 3.

In Figure 17, the change of pile diameter and length is shown in relation with the cost and CO₂ emission values for all envisaged cases. The pile diameter and length remain approximately the same for all the cases and the change against the excavation depth remains constant too. This situation causes the acquisition of a constant minimum cross section and ensures the minimalistic approach to design. As a result of using constant values for material costs, the total cost is protected and only the change of the CO₂ emission values of materials becomes important in the evaluation process of a sustainable design. The logic of the design process is similar for all the solutions conducted by four different kinds of objectives.

In Figure 18, the change of the numbers and diameters of the reinforcing bars is given together with the change of related total cost and CO₂ emission for all cases. It is clear that in Figure 18, since the main logic in the purpose functions is to achieve the smallest amount of CO₂ emissions integrated with minimum cost, changes in the diameter and number of reinforcements occur in piles of the same diameter and length in order to ensure geotechnical stability and fulfil structural strength requirements. The number and diameter of reinforcing bars affect the content of the reinforced concrete design and, therefore, the relationship between the minimization processes of the CO₂ emission. The optimization process includes minimizing the emission with the balance of the wasting materials hence a visual rate between the selected number and diameter of the reinforcing bars cannot be obtained in all cases.

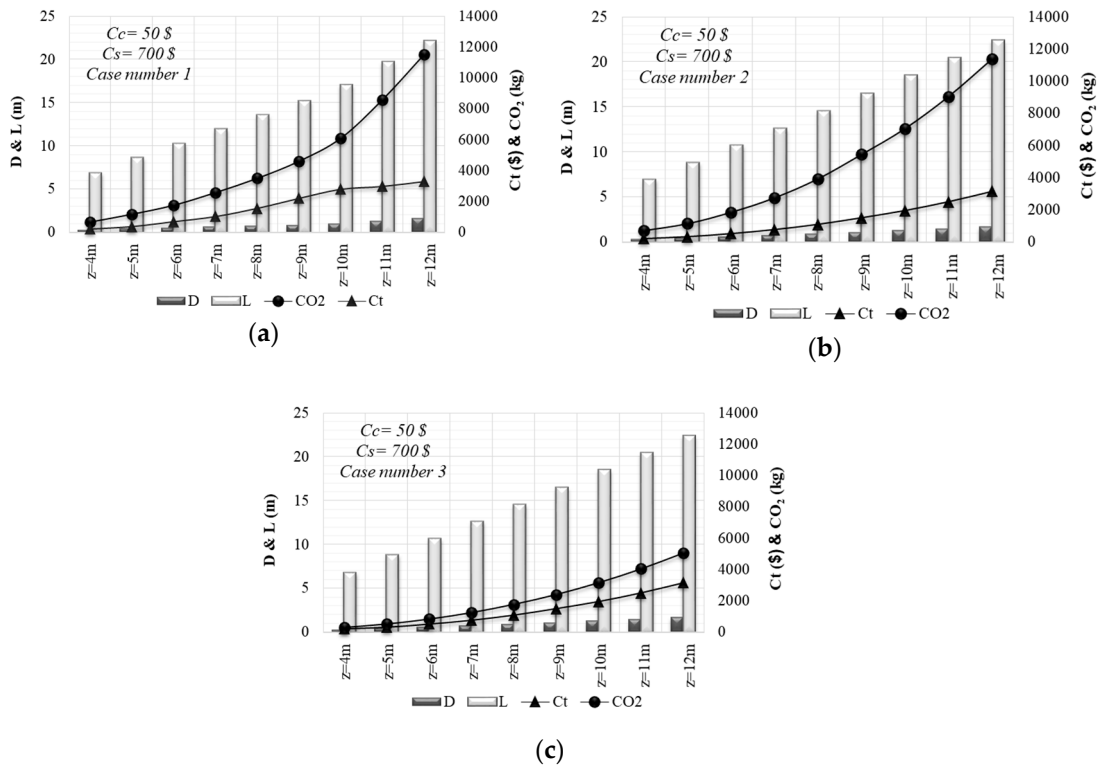


Figure 17. The change of pile diameter and length against total cost and CO₂ emission ($C_c = \$50$, $C_s = \$700$). (a) Case 1; (b) Case 2; (c) Case 3.

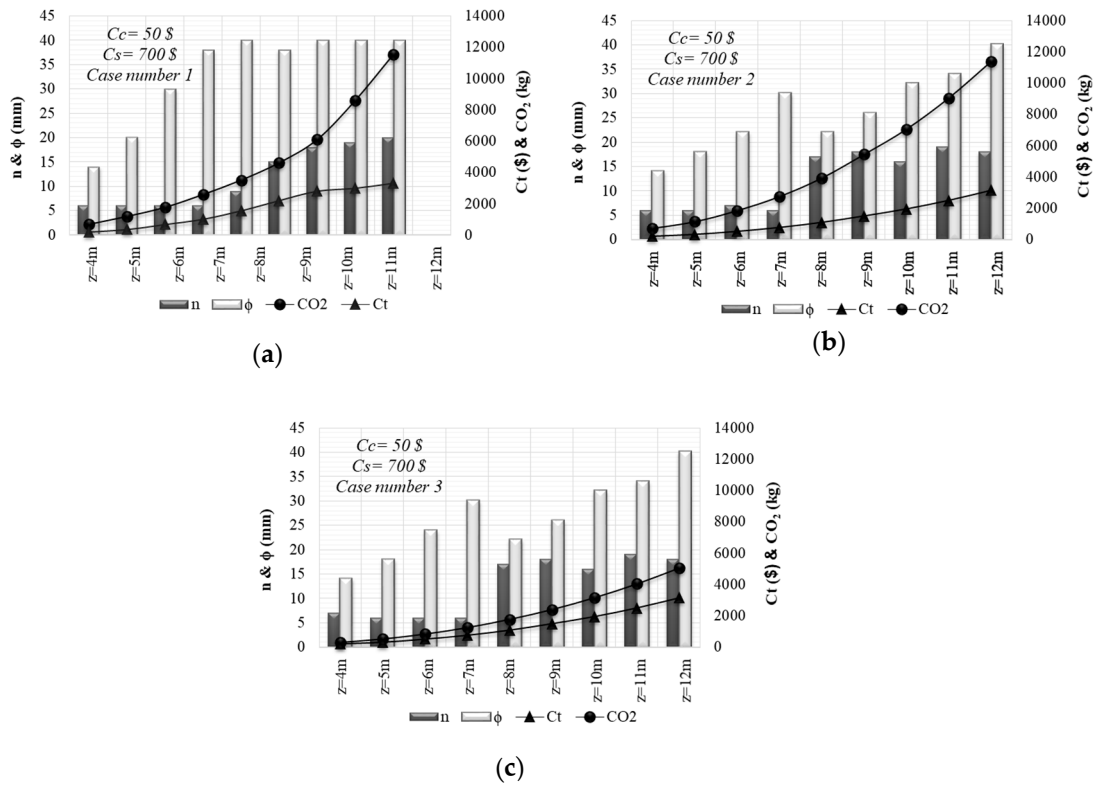


Figure 18. The change of the diameter and number of reinforcing bars against total cost and CO₂ emission ($C_c = \$50$, $C_s = \$700$) (a) Case 1; (b) Case 2; (c) Case 3.

5. Conclusions

Within the context of this study, the Harmony Search Algorithm is used to calculate the minimization relationship between the cost and the CO₂ emissions for the cantilever soldier pile wall systems via the performance of four different objectives. Therefore, 2251 parametrical analyses were conducted to examine the appropriateness of the use of the Harmony Search Algorithm for the design process of the cantilever soldier pile walls. The piles are assumed to be embedded in a constant type of pure frictional soil formation and Rankine's earth pressure theory is used to calculate the lateral earth trust caused by the soil mass. The design of the cantilever pile system is performed with the use of beams on elastic soil assumption and the pile diameter is selected as one of the variants of the analyses. The embedment depths in relation with the envisaged different excavation depths are also investigated at the design step of the analyses. Four different objective functions are prepared to survey the minimization process between optimum design, minimum cost and CO₂ emission. The first function is defined to search for the effects of the minimum cost quest against optimum dimensions. The second function is performed to acquire the most environmentally friendly solution for the construction of retaining structures. The third function is prepared to search for the appropriateness of the use of the cost and CO₂ emission minimization target together with the optimal dimensions. The last function is arranged to investigate the compatibility of the cost and emission by utilizing a well-accepted study of the literature.

The results of the analysis demonstrate that the most effective factor of the design of cantilever soldier piles is the depth of excavation. The diameter and the length of the pile is identified directly by the excavation depth. Therefore, the most significant factor of cost minimization has to be the selection of proper cross section of pile to resist the lateral earth trust caused by the envisaged depth. The increase of the depth of excavation also induces an increase in the length of the pile. This condition directly leads to an enhancement of the volume of construction materials and the increment of the CO₂ distribution caused by both concrete and steel. The outcomes of the study present the mentioned ordered relationship between design-cost and emission with the use of graphical comparisons. The comparisons are special due to the use of cantilever soldier piles as the investigated structure.

Figure 19 was created to search for the results of different objective functions in relation to the change of the total cost against excavation depth. The abbreviation OF is used to identify objective functions in the illustrations of the design. In Figure 20, the results of the objective functions are presented according to the CO₂ emission values.

In Figures 19 and 20, the costs of the materials are assumed to be constant in all the cases taken into consideration ($C_c = \$50$, $C_s = \$700$) and objective functions 2–4 are investigated with consideration of the envisaged 3 different cases. It is a clear situation that only the consideration of CO₂ emissions in the objective function with a high emission value of concrete leads to an increase in the total cost of the construction. The increase of steel emission value cannot affect the design. This means that the procurement of lower CO₂ emissions can be possible by using higher amounts of steel material. The increase of the pile depth in relation to the depth of excavation causes the objective functions to evaluate the same cost value depending on the achievement of the same cross section to ensure stability. The relative difference between the costs obtained by the performance of different functions is also decreased based on the increase of excavation depth. Considering Figure 20, it can be said that the minimum emission value of CO₂ is obtained in the third cases of all envisaged objective functions. Case 3 is differentiated from others by the use of low emission values of the construction materials. Besides, the comparison of the other emission values exhibits a similar trend for the same excavation depth. The use of objective function 1, in other words, the use of only a material minimization process in the design, tends to exhibit similar emission values with the other objective function solutions for Cases 1 and 2. This is an important result that has to be taken into consideration in the selection of construction materials. The acquisition of an environmentally friendly design for sustainable usage also necessitates the selection of materials that are especially harmless to living beings. Otherwise, the use of special optimization techniques cannot ensure the minimization of CO₂ emissions.

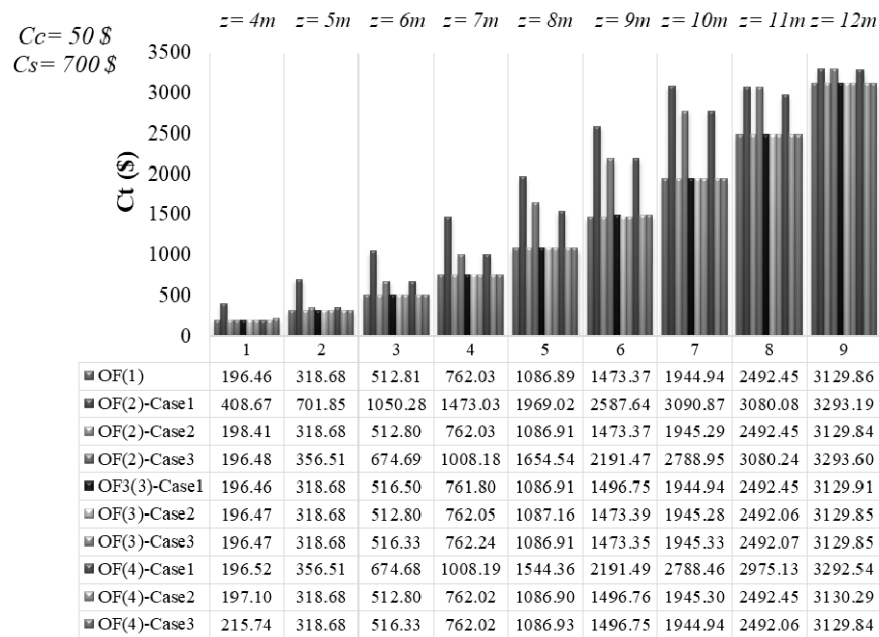


Figure 19. The total cost values against the excavation depth via different objective functions ($C_c = \$50$, $C_s = \$700$).

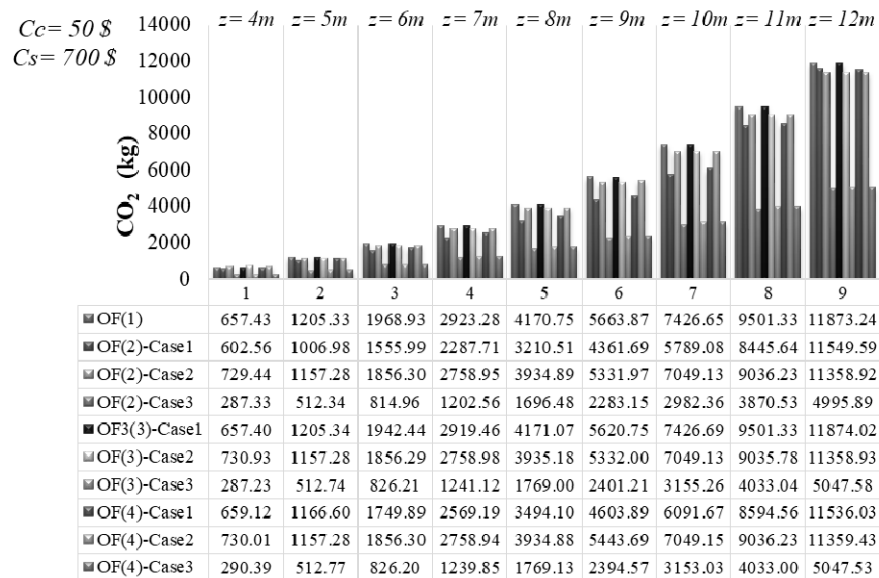


Figure 20. The CO₂ emission values against the excavation depth via different objective functions ($C_c = \$50$, $C_s = \$700$).

Figure 21 is also compiled to search for the results of different objective functions in relation with the change of the total cost against excavation depth. In Figure 22, the results of the objective functions are presented according to the CO₂ emission values. In Figures 21 and 22, the costs of the materials are assumed to be constant in all the cases taken into consideration ($C_c = \$150$, $C_s = \$1100$) and objective functions 2–4 are investigated considering the envisaged 3 different cases. The outcomes of the study are similar to the analysis conducted for the situation evaluated in Figures 19 and 20.

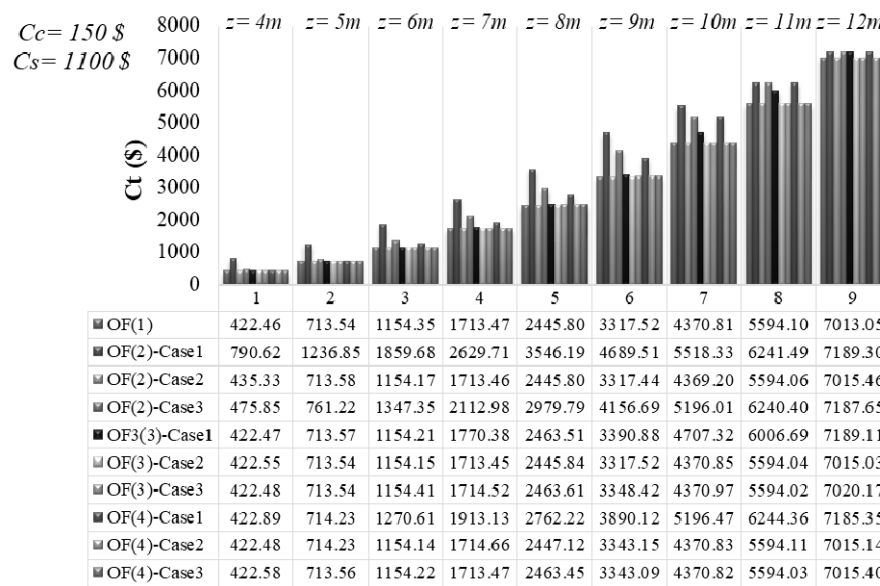


Figure 21. The total cost values against the excavation depth via different objective functions ($C_c = \$150$, $C_s = \$1100$).

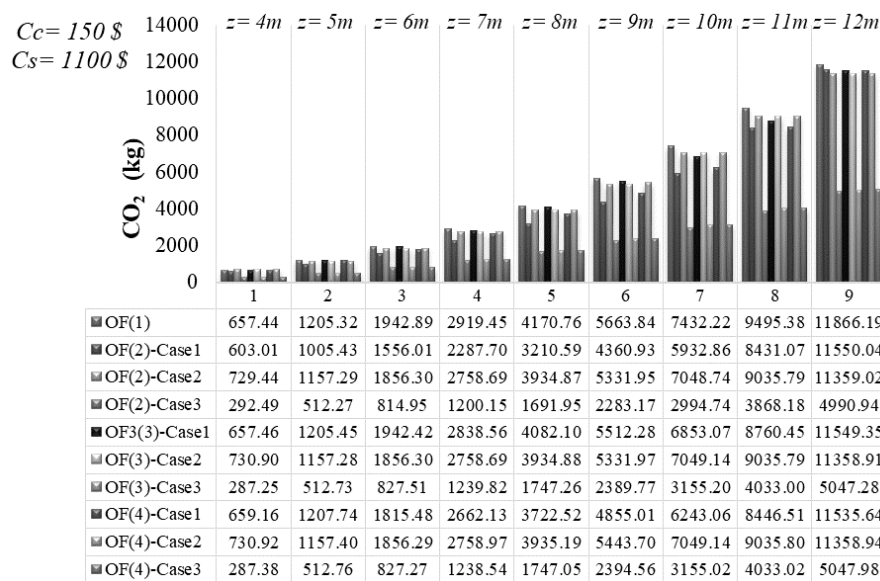


Figure 22. The CO₂ emission values against the excavation depth via different objective functions ($C_c = \$150$, $C_s = \$1100$).

It can be seen from the comparison between Figures 19 and 21 that the relative difference between the total costs decreases with the increase of the costs of the materials. But the cost increases of the materials are not equal. The rise of concrete cost is three times the first cost of the concrete, but the rise of steel is only by 60%. This non-proportional increase of the cost of the concrete causes costs to hit their peak because the volume of the concrete that is used to construct the pile seems to be a more significant factor for the emission and cost than steel weight. As a result, the significant point of the analysis conducted to search for the harmony between the cost and CO₂ emissions shows that the design of cantilever soldier piles, also considering the minimization process of CO₂ emissions, does not have a material effect on the optimum cost of the pile wall system. Hence, it is admissible to use the objective function that considers the relationship of both cost and emission at the design stage of the cantilever soldier piles.

Consequently, this study focuses on the optimal design details of the cantilever soldier piles considering the sustainable design requirements. The number of studies related to the sustainable design of the cantilever soldier piles is really limited in the literature. Therefore, it is thought that this study compensates for a major deficiency in the design process of piled retaining systems. Besides, the significant and effective factors of design are addressed throughout the conducted optimization analyses to show the attainment of both cost and CO₂ emission minimization. Thus, this paper can be beneficial for both engineers and researchers to develop new insights into obtaining both cost-effective and eco-friendly design approaches.

Author Contributions: G.B. and A.E.K. generated the analysis codes. G.B., A.E.K., and Z.A.A. developed the theory background and formulations of the system. The text of the paper was formed by Z.A.A. and G.B., Z.W.G. supervised the research direction. All authors have read and agreed to the published version of the manuscript.

Funding: This work was supported by the National Research Foundation of Korea (NRF) grant funded by the Korea government (MSIT) (2020R1A2C1A01011131). This research was also supported by the Energy Cloud R&D Program through the National Research Foundation of Korea (NRF) funded by the Ministry of Science, ICT (2019M3F2A1073164).

Conflicts of Interest: The authors declare no conflict of interest.

References

1. Azizi, F. *Applied Analyses in Geotechnics*; E & FN Spon: London, UK; Taylor and Francis Group: New York, NY, USA, 1999; ISBN 9780419253501.
2. Das, B.M. *Principles of Foundation Engineering*, 6th ed.; Thomson: Toronto, ON, Canada, 2007; ISBN 9781305081567.
3. Lee, C.J.; Wei, Y.C.; Chen, H.T.; Chang, Y.Y.; Lin, Y.C.; Huang, W.S. Stability analysis of cantilever double soldier-piled walls in sandy soil. *J. Chin. Inst. Eng.* **2011**, *34*, 449–465. [[CrossRef](#)]
4. Macnab, A. *Earth Retention Systems Handbook*; McGraw-Hill: New York, NY, USA, 2002; pp. 319–322, ISBN 978-0071373319.
5. Lyndon, A.; Pearson, R.A. Pressure distribution on a rigid retaining wall in cohesionless material. In Proceedings of the Symposium Application of Centrifuge Modeling to Geotechnical Design, Manchester, UK, 16–18 April 1984; pp. 271–280.
6. Clayton, C.R.I.; Militisky, J. *Earth Pressure and Earth Retaining Structures*; Blackie Academic & Professional: New York, NY, USA, 1993; ISBN 9781138427297.
7. Randolph, M.F. The response of flexible piles to lateral loading. *Geotechnique* **1981**, *31*, 247–259. [[CrossRef](#)]
8. Verruijt, A.; Kooijman, A.P. Laterally loaded piles in a layered elastic medium. *Geotechnique* **1989**, *39*, 39–49. [[CrossRef](#)]
9. Konagai, K.; Yin, Y.; Murono, Y. Single beam analogy for describing soil–pile group interaction. *Soil Dyn. Earthq. Eng.* **2003**, *23*, 31–39. [[CrossRef](#)]
10. Rashidi, F.; Shahir, H. Numerical investigation of anchored soldier pile wall performance in the presence of surcharge. *Int. J. Geotech. Eng.* **2019**, *13*, 162–171. [[CrossRef](#)]
11. Aydoğdu, İ.; Akın, A. Biogeography Based CO₂ and Cost Optimization of RC Cantilever Retaining Walls. *World Acad. Sci. Eng. Technol. Int. J. Civil Environ. Eng.* **2015**. [[CrossRef](#)]
12. Villalba, P.; Alcalá, J.; Yepes, V.; Gonzales-Vidosa, F. CO₂ optimization of reinforced concrete cantilever retaining walls. In Proceedings of the 2nd International Conference on Engineering Optimization, Lisbon, Portugal, 6–9 September 2010.
13. Sasidhar, T.; Neeraja, D.; Sudhindra, V.S.M. Application of genetic algorithm technique for optimizing design of reinforced concrete retaining wall. *Int. J. Civ. Eng. Technol.* **2017**, *8*, 999–1007.
14. Goldberg, D.E. *Genetic Algorithms in Search, Optimization and Machine Learning*; Addison Wesley: Boston, MA, USA, 1989; ISBN 978-0201157673.
15. Holland, J.H. *Adaptation in Natural and Artificial Systems*; University of Michigan Press: Ann Arbor, MI, USA, 1975; ISBN 9780262082136.
16. Kaveh, A.; Kalateh-Ahani, M.; Fahimi-Farzam, M. Constructability optimal design of reinforced concrete retaining walls using a multi-objective genetic algorithm. *Struct. Eng. Mech.* **2013**, *47*, 227–245. [[CrossRef](#)]
17. Kennedy, J.; Eberhart, R.C. Particle swarm optimization. In Proceedings of the IEEE International Conference on Neural Networks No. IV, Perth, Australia, 27 November–1 December 1995; pp. 1942–1948.

18. Ahmadi-Nedushan, B.; Varaee, H. Optimal Design of Reinforced Concrete Retaining Walls using a Swarm Intelligence Technique. In Proceedings of the First International Conference on Soft Computing Technology in Civil, Structural and Environmental Engineering, Stirlingshire, Scotland, 1 September 2009.
19. Yang, X.S. *Firefly Algorithms for Multimodal Optimization*; In Stochastic Algorithms: Foundations and applications; Springer: Berlin/Heidelberg, Germany, 2009; pp. 169–178.
20. Sheikholeslami, R.; Khalili, B.G.; Zahrai, S.M. Optimum Cost Design of Reinforced Concrete Retaining Walls Using Hybrid Firefly Algorithm. *Int. J. Eng. Technol.* **2014**, *6*, 465–470. [[CrossRef](#)]
21. Erol, O.K.; Eksin, I. A new optimization method: Big bang–big crunch. *Adv. Eng. Softw.* **2006**, *37*, 106–111. [[CrossRef](#)]
22. Camp, C.V.; Akin, A. Design of Retaining Walls Using Big Bang-Big Crunch Optimization. *J. Struct. Eng. ASCE* **2012**, *138*, 438–448. [[CrossRef](#)]
23. Geem, Z.W.; Kim, J.H.; Loganathan, G.V. A new heuristic optimization algorithm: Harmony search. *Simulation* **2001**, *76*, 60–68. [[CrossRef](#)]
24. Kaveh, A.; Abadi, A.S.M. Harmony search based algorithms for the optimum cost design of reinforced concrete cantilever retaining walls. *Int. J. Civ. Eng.* **2011**, *9*, 1–8.
25. Yang, X.S. A New Metaheuristic Bat-Inspired Algorithm. In *Nature Inspired Cooperative Strategies for Optimization (NISCO 2010)*; Studies in Computational Intelligence; Springer: Berlin/Heidelberg, Germany, 2010; pp. 65–74. [[CrossRef](#)]
26. Talatahari, S.; Sheikholeslami, R. Optimum design of gravity and reinforced retaining walls using enhanced charged system search algorithm. *KSCE J. Civ. Eng.* **2014**, *18*, 1464–1469. [[CrossRef](#)]
27. Ceranic, B.; Fryer, C.; Baines, R.W. An application of simulated annealing to the optimum design of reinforced concrete retaining structures. *Comput. Struct.* **2001**, *79*, 1569–1581. [[CrossRef](#)]
28. Yepes, V.; Alcalá, J.; Perea, C.; Gonzalez-Vidosa, F. A parametric study of optimum earth-retaining walls by simulated annealing. *Eng. Struct.* **2008**, *30*, 821–830. [[CrossRef](#)]
29. Pei, Y.; Xia, Y. Design of cantilever retaining walls using heuristic optimization algorithms. *Procedia Earth Planet. Sci.* **2012**, *5*, 32–36. [[CrossRef](#)]
30. Mergos, P.E.; Mantoglou, F. Optimum design of reinforced concrete retaining wall with the flower pollination algorithm. *Struct. Multidiscip. Optim.* **2019**. [[CrossRef](#)]
31. Yoo, D.G.; Kim, J.H.; Geem, Z.W. Overview of harmony search algorithm and its applications in civil engineering. *Evol. Intell.* **2014**, *7*, 3–16. [[CrossRef](#)]
32. Geem, Z.W. *State-of-the-Art in the Structure of Harmony Search Algorithm, Recent Advances in Harmony Search Algorithm*; Springer: Berlin/Heidelberg, Germany, 2010; Volume 270, pp. 1–10. [[CrossRef](#)]
33. Akin, A.; Saka, M.P. Optimum Design of Concrete Cantilever Retaining Walls Using the Harmony Search Algorithm. In *Proceedings of the Tenth International Conference on Computational Structures Technology*; Topping, B.H.V., Adam, J.M., Pallarés, F.J., Bru, R., Romero, M.L., Eds.; Civil-Comp Press: Stirlingshire, UK, 2010; p. 130. [[CrossRef](#)]
34. Molina-Moreno, F.; García-Segura, T.; José, V.M.; Yepes, V. Optimization of buttressed earth-retaining walls using hybrid harmony search algorithms. *Eng. Struct.* **2017**, *134*, 205–216. [[CrossRef](#)]
35. Yepes, V.; Martí, J.V.; Garcia, J. Black hole algorithm for sustainable design of counterfort retaining walls. *Sustainability* **2020**, *12*, 2767. [[CrossRef](#)]
36. Aydoğdu, İ. Comparison of metaheuristics on multi objective (cost&CO₂) optimization of RC cantilever retaining walls. *Pamukkale Univ. Muh. Bilim. Derg.* **2017**, *23*, 221–231. [[CrossRef](#)]
37. Khajezadeh, M.; Taha, M.R.; Eslami, M. Efficient gravitational search algorithm for optimum design of retaining walls. *Struct. Eng. Mech.* **2013**, *45*, 111–127. [[CrossRef](#)]
38. Öztürk, H.T.; Türkeli, E. Optimum design of RC Retaining walls with key section using jaya algorithm. *J. Polytech* **2019**, *22*, 283–291. [[CrossRef](#)]
39. King, G.J.W. Analysis of cantilever sheet-pile walls in cohesionless soil. *J. Geotech. Eng.* **1995**, *121*, 629–635. [[CrossRef](#)]
40. Bica, A.V.D.; Clayton, C.R.I. Limit equilibrium design methods for free embedded cantilever walls in granular soils. *Proc. Inst. Civ. Eng.* **1989**, *86*, 879–898. [[CrossRef](#)]
41. Banerjee, P.K.; Davies, T.G. The behaviour of axially and laterally loaded single piles embedded in nonhomogeneous soils. *Géotechnique* **1978**, *28*, 309–326. [[CrossRef](#)]

42. Kay, S.; Griffiths, D.V.; Kolk, H.J. Application of pressuremeter testing to assess lateral pile response in clays. In *Pressuremeter and Its Marine Applications: Second International Symposium*; Briaud, J., Audibert, J., Eds.; ASTM International: West Conshohocken, PA, USA, 1985. [[CrossRef](#)]
43. Geem, Z.W.; Lee, K.S.; Park, Y. Application of harmony search to vehicle routing. *Am. J. Appl. Sci.* **2005**, *2*, 1552–1557. [[CrossRef](#)]
44. Ulusoy, S.; Kayabekir, A.E.; Bekdaş, G.; Niğdeli, S.M. Metaheuristic Algorithms in Optimum Design of Reinforced Concrete Beam by Investigating Strength of Concrete. *Chall. J. Concr. Res. Lett.* **2020**, *11*, 33–37. [[CrossRef](#)]
45. Ulusoy, S.; Kayabekir, A.E.; Bekdaş, G.; Niğdeli, S.M. Optimum Design of Reinforced Concrete Multi-Story Multi-Span Frame Structures under Static Loads. *Int. J. Eng. Technol.* **2018**, *10*, 403–407. [[CrossRef](#)]
46. ACI Committee 318. *Building Code Requirements for Structural Concrete (ACI 318-14) and Commentary on Building Code Requirements for Structural Concrete (ACI 318R-14)*; American Concrete Institute: Farmington Hills, MI, USA, 2014.
47. Gajan, S. Normalized relationships for depth of embedment of sheet pile walls and soldier pile walls in cohesionless soils. *Soils Found* **2011**, *51*, 559–564. [[CrossRef](#)]
48. FHWA-IF-99-015. *Geotechnical Engineering Circular No. 4 Ground Anchors and Anchored Systems*; Federal Highway Administration: Washington, DC, USA, 1999.
49. *Kazı Çukurlarının Stabilitesi ve İksa Sistemi Etüt, Proje, Uygulama ve Kontrolleri İle İlgili Uygulacak Esaslar hakkında Kazı Güvenliği ve Alınacak Önlemler*; Çevre ve şehircilik Bakanlığı: Ankara, Turkey, 2018.
50. British Standards Institution. *Eurocode 7: Part 1, General Rules*; British Standards Institution: London, UK, 1995.
51. Yeo, D.; Potra, F.A. Sustainable design of reinforced concrete structures through CO₂ emission optimization. *J. Struct. Eng.* **2015**, *141*, B4014002. [[CrossRef](#)]
52. Paya-Zaforteza, I.; Yepes, V.; Hospitaler, A.; Gonzalez-Vidosa, F. CO₂-optimization of reinforced concrete frames by simulated annealing. *Eng. Struct.* **2009**, *31*, 1501–1508. [[CrossRef](#)]
53. Bekdaş, G.; Akbay Arama, Z.; Kayabekir, A.E.; Geem, Z.W. Optimal design of cantilever soldier pile retaining walls embedded in frictional soils with harmony search algorithm. *Appl. Sci.* **2020**, *10*, 3232. [[CrossRef](#)]



© 2020 by the authors. Licensee MDPI, Basel, Switzerland. This article is an open access article distributed under the terms and conditions of the Creative Commons Attribution (CC BY) license (<http://creativecommons.org/licenses/by/4.0/>).